ELSEVIER

Journal of Molecular Structure 444 (1998) 135–146

Journal of
MOLECULAR
STRUCTURE

Structure and nonlinear optical properties of phenylazo compounds. Structural characterization of 3-amino-3-morpholinyl-2-(*o*-nitrophenylazo)-propenonitrile and *o*-nitrophenylhydrazonomalononitrile

Vladimir N. Nesterov[a], Tatiana V. Timofeeva[b], Gary Duerksen[b], Ronald D. Clark[b]

[a]*Institute of Organoelement Compounds, Russian Academy of Sciences, 117813, Moscow, Russia*
[b]*School of Physical Sciences, New Mexico Highlands University, Las Vegas, NM 87701 USA*

Received 19 May 1997; accepted 29 September 1997

Abstract

The results of synthesis, X-ray and spectral investigations, powder second harmonic generation (SHG), molecular mechanics and quantum chemical calculations of the potential nonlinear optical compound, 3-amino-3-morpholinyl-2-(*o*-nitrophenylazo)-propenonitrile (I) and its synthetic precursor *o*-nitrophenylhydrazonomalononitrile (II) are presented. The interrelations of molecular structure and crystal packing characteristics, important for SHG prediction, are discussed on the basis of molecular mechanics dimer structure calculations and the results of X-ray investigations. The conclusions about the low probability of SHG by compound I in the crystal form, in spite of its high calculated molecular hyperpolarizability value, are confirmed by powder SHG measurements. © 1998 Elsevier Science B.V.

Keywords: Azo-compounds; NLO properties; X-ray analysis; Molecular mechanics

1. Introduction

The present article is part of a program of synthesis, X-ray and spectral investigations, molecular mechanics and quantum chemical calculations, of compounds with nonlinear optical properties. The majority of organic compounds exhibiting large SHG (second harmonic generation) efficiencies are polarizable dipolar molecules with a π-conjugated electron donor–acceptor arrangement [1,2]. These requirements are fulfilled with donor–acceptor substituted polyene compounds. According to quantum chemical calculations [3] the –C=C– bridge has high SGH efficiency, while the efficiency of the –N=N– bridge is slightly less in such systems. In the present work we started structural investigations of molecules with a combination of both these types of bridges.

Using the previously mentioned requirements of molecular structure it is possible to predict SHG only in solution. It is well known that SHG in the crystalline state can be observed only for non-centrosymmetrical media [1]. Unfortunately, prediction of the type of crystalline symmetry for specific molecules is not understood completely (see for instance Refs. [4,5]). So, for the example of the compounds under investigation, we also tried to find interrelations between the molecular and crystalline structure. This was done by modeling of the molecular dimer structures and analysis of the relations between symmetry of the isolated molecular dimer and most

PII S0022-2860(97)00374-8

stable molecular associates in the crystal form. Calculations of this type have been done before for nonlinear materials including *m*-nitroaniline (mNA) and some other organic molecules [6,7] and *o*-methoxydicyanovinylbenzene (DIVA) and its derivatives [8].

We present the results of molecular mechanics and quantum chemical calculations, X-ray study and some spectral investigations of the potential nonlinear optical compound 3-amino-3-morpholinyl-2-(*o*-nitrophenylazo)-propenonitrile (I) and its precursor in the synthesis process, *o*-nitrophenylhydrazonomalononitrile (II).

2. Experimental part and calculation details

2.1. Materials

o-Nitrophenylhydrazonomalononitrile (II) was prepared from *o*-nitroanilinediazonium salt with malononitrile using the standard procedure described in articles [9–11]. The yield of compound II was ca. 80%, (m.p. 144–146°). 1H NMR ($CDCl_3$) (δ; 7.39 (1H, t.d, C_4H), 7.80 (1H, t.d, C_5H), 7.95 (1H, d.d, C_6H), 8.33 (1H, d.d, C_3H), 12.6 (1H, s, NH). 3-Amino-3-morpholinyl-2-(*o*-nitrophenylazo)-propenonitrile (I) was prepared by the following procedure. To an ethanol solution of 3 mmol of compound II 3 mmol of morpholine under stirring was added. The solution was kept at room temperature 12 h. The solvent was removed and orange crystals were washed with ethanol and hexane. The yield of compound I was ca. 94%. ^1H NMR ($CDCl_3$) δ: 3.68 (4H, t, CH_2), 3.78 (4H, t, CH_2), 6.6 (2H, w.s, NH_2), 7.25 (1H, t.d, C_4H), 7.53 (1H, t.d, C_5H), 7.64 (2H, m, C_3H, C_6H). Both compounds were recrystallized from ethanol until they showed no impurities as shown by thin layer chromatography on Silufol UV-254 plates using acetone–hexane (3:5) for elution.

2.2. X-ray analysis

Single crystals of I and II suitable for X-ray analysis were obtained by slow evaporation from ethanol. Single crystalline samples of I are orange needles; samples of II are yellow needles. The experimental data were obtained at room temperature (I) and low temperature (II) using Mo Kα radiation and a graphite monochromator (λ = 0.7107 Å) with the 4-circle automatic diffractometers Siemens P3/PC (I) and "Syntex $P2_1$" (II) using the $\theta/2\theta$-scan technique. The structures were solved by direct methods and refined by a full-matrix least-squares procedure in the anisotropic–isotropic (hydrogen atoms) approximation, and refined with 1970 (I) and 1790 (II) reflections with $I > 3\sigma(I)$. All hydrogen atoms were unambiguously located on a difference Fourier map and refined in isotropic approximation for structure I. Isotropic refinement was done in structure II only for the hydrogen atoms of the NH_2 group, all other hydrogen atoms, because of the large values for thermal motion factors, were included in refinement (riding model) with fixed positional thermal parameters U = 0.05 Å^2. All calculations were carried out with a personal computer using the SHELXTL PLUS program package [12]. Important details of the data collection and structure refinement are summarized in Table 1. Coordinates of non-hydrogen atoms and their isotropic equivalent displacement parameters are given in Tables 2 and 3. Bond lengths, bond angles and some torsion angles are presented in Tables 4 and 5.

2.3. Powder SHG and absorption spectrum measurements

The sample of compound I was screened for SHG ($\chi^{(2)}$) using the technique of Kurtz [13]. The refractive index of the material was determined by the Becke line method to be 1.76; the sample was sifted through a 75 μm sieve with a sonic sifter and loaded into a cell made by sandwiching a 250 μm thick void between two 150 μm thick face plates of ordinary glass; light scatter from the sample was minimized by immersing the powder in an index-matching fluid in the cell; the cell was illuminated by the fundamental (1064 nm) output from a Nd:YAG laser; SHG was measured as 532 nm light output.

The experimental configuration is depicted in Fig. 1. The samples were illuminated with the quasi-CW output of a Quantronix 116 mode-locked Nd:YAG laser operating at 10 W and producing 70 ps pulses every 10 ns—at the test settings the peak pulse power was about 1500 W. The laser beam was interrupted by a mirrored chopper and alternately focused to a beam diameter of approximately 3 mm on the sample or a

Table 1
Structure determination summary for compounds I and II

		I	II
Empirical formula		$C_{13}H_{14}N_6O_3$	$C_9H_5N_5O_2$
Formula weight		302.3	215.2
Crystal size (mm)		0.2 × 0.3 × 0.2	0.2 × 0.3 × 0.2
Crystal system		monoclinic	monoclinic
Space group		$P2_1$	$P2_1/n$
Z		4	4
Unit cell dimensions	a (Å)	7.465(4)	8.821(2)
	b (Å)	12.440(6)	5.695(2)
	c (Å)	16.085(7)	19.186(6)
	β (°)	98.69(4)	96.42(2)
Volume (Å^3)		1477(1)	957.8(5)
Density (calc.) (g cm^{-3})		1.360	1.492
Absorption coefficient (mm^{-1})		0.101	0.113
F(000)		632	440
Diffractoimeter used		Siemens P3/PC	Syntex $P2_1$
Temperature (K)		297	193
2θ Range (°)		2.0–56	2.0–54
Scan range (ω, °)		1.80	1.80
No. reflections collected		3296	2476
No. independent reflections		3057	2329
No. observed reflections ($F > 6.0\sigma$)		1970	1790
No. parameters refined		408	165
Empirical extinction correction		N/A	N/A
Data-to-parameters ratio		4.8:1	10.8:1
Final R indices (obs. data)		5.56%	3.88%
Final wR indices (obs. data)		5.22%	3.75%
Goodness-of-fit		0.85	0.45
Largest difference peak (e Å^{-3})		0.34	0.21
Largest difference hole (e Å^{-3})		0.00	− 0.16

reference cell of MNA after passing through a long-pass filter. The transmitted light was analyzed using a 532 nm bandpass interference filter and detected with a Hamamatsu HC-120 photomultiplier assembly. The output from each PMT was supplied to a lock-in amplifier referenced to the chopper frequency. All experimental control and data-capture was integrated via GPIB bussing and using LabVIEW software.

The experimental parameters were chosen so that the sample thickness exceeded the average grain size by an order of magnitude, and the beam diameter exceeded the sample thickness by an order of magnitude. These relations ensured that the measurements represented a random average over particle orientations and inhomogeneities in the sample density.

The electronic absorption spectrum of compound I was measured in an ethanol solution with a Hewlett Packard 8453 UV–VIS spectrometer using a deuterium and hydrogen lamp.

2.4. Molecular mechanics calculations

Calculations of the conformation and geometry of the experimentally studied molecules I and II in a free state were performed using the MM3 program package [14,15]. The energy of molecular dimers was also calculated with MM3 using the stochastic search procedure [16]. The total energy being calculated as a sum of the intra- and intermolecular interactions. The advantage of the stochastic procedure in comparison with mapping of intermolecular energy (as a function of interplanar distance and in-plane rotation angle) described by Itoh et al. [6,7], is that molecular conformations and relative molecular positions in dimers were not restricted during optimization. As the starting points for a stochastic search three possible dimers were taken with the parallel, centrosymmetric C_i, and C_2-symmetry mutual molecular orientations. In most cases dimers

Table 2
Atom coordinates (× 10^4) and equivalent isotropic displacement coefficients ($Å^2 \times 10^3$) in molecule I

Atom	x	y	z	U(eq) [a]
O(17)	699(6)	9315	7410(3)	63(2)
O(21)	4567(10)	3859(6)	4504(5)	109(3)
O(22)	6472(8)	2913(9)	5315(6)	159(4)
N(7)	2632(6)	4067(4)	6001(3)	45(2)
N(8)	1242(6)	4541(4)	6216(3)	38(2)
N(11)	4814(7)	6255(5)	6893(4)	62(2)
N(13)	- 1376(6)	5532(4)	6929(3)	45(2)
N(14)	24(6)	7172(4)	6873(3)	44(2)
N(20)	4961(9)	3178(6)	5013(5)	70(3)
C(1)	2262(7)	3004(5)	5722(4)	41(2)
C(2)	3481(8)	2513(6)	5276(4)	50(2)
C(3)	3362(9)	1442(6)	5036(4)	57(3)
C(4)	1953(10)	828(6)	5231(4)	60(3)
C(5)	684(9)	1304(6)	5664(4)	57(3)
C(6)	820(9)	2374(5)	5908(4)	50(2)
C(9)	1557(7)	5555(5)	6531(4)	39(2)
C(10)	3326(7)	5952(5)	6713(4)	41(2)
C(12)	32(7)	6105(5)	6784(3)	33(2)
C(15)	990(8)	7936(5)	6398(4)	47(2)
C(16)	1953(9)	8759(6)	6981(5)	60(3)
C(18)	- 158(9)	8584(5)	7897(4)	56(3)
C(19)	- 1214(8)	7735(6)	7363(4)	54(2)
O(17')	5791(6)	72(4)	8024(3)	71(2)
O(21')	- 589(14)	5684(10)	10349(5)	197(6)
O(22')	- 1606(9)	6135(10)	9198(8)	219(7)
N(7')	2056(6)	5224(4)	8889(3)	42(2)
N(8')	3421(6)	4750(4)	8672(3)	40(2)
N(11')	- 219(7)	3144(5)	7914(4)	59(2)
N(11')	6007(7)	3857(5)	7899(4)	46(2)
N(14')	4554(6)	2219(4)	7794(3)	40(2)
N(20')	- 386(9)	6166(6)	9792(5)	77(3)
C(1')	2524(8)	6248(5)	9256(4)	44(2)
C(2')	1276(8)	6740(5)	9690(4)	47(2)
C(3')	1535(10)	7753(6)	10062(4)	61(3)
C(4')	3111(11)	8289(6)	9986(5)	62(3)
C(5')	4382(10)	7827(6)	9555(5)	62(3)
C(6')	4102(8)	6836(6)	9184(4)	52(2)
C(9')	3086(7)	3776(5)	8284(4)	38(2)
C(10')	1277(8)	3396(5)	8088(4)	43(2)
C(12')	4577(7)	3248(5)	7993(4)	38(2)
C(15')	3410(9)	1404(5)	8113(5)	54(2)
C(16')	4645(9)	531(6)	8562(5)	59(3)
C(18')	6914(9)	887(6)	7753(5)	68(3)
C(19')	5792(8)	1742(6)	7261(4)	52(2)

[a] Equivalent isotropic U defined as one third of the trace of the orthogonalized $U_{i,j}$ tensor

retained the initial molecular orientation during the optimization process but not the starting molecular positions. The top-list of the dimer energies, found as a result of stochastic search are presented in Table 6.

2.5. Calculations of static polarizabilities (β)

For the computation of second order polarizabilities a modification of the static field method [17] developed in [18,19] was used. 252 static-field calculations

Table 3
Atom coordinates ($\times 10^4$) and equvalant isotropic displacement coefficients ($\text{Å}^2 \times 10^3$) in molecule II

Atom	x	y	z	U(eq) [a]
O(1)	2267(1)	- 47(2)	1714(1)	38(1)
O(2)	594(1)	- 51(2)	809(1)	45(1)
N(1)	1727(1)	- 883(2)	1144(1)	31(1)
N(2)	4229(1)	- 3421(2)	1916(1)	28(1)
N(3)	5367(1)	- 4556(2)	2263(1)	27(1)
N(4)	5044(2)	428(3)	3225(1)	43(1)
N(5)	8182(2)	- 5577(3)	3614(1)	38(1)
C(1)	3626(2)	- 4154(3)	1248(1)	26(1)
C(2)	2437(2)	- 2914(3)	864(1)	28(1)
C(3)	1852(2)	- 3651(3)	194(1)	34(1)
C(4)	2434(2)	- 5594(3)	- 95(1)	38(1)
C(5)	3605(2)	- 6834(3)	281(1)	36(1)
C(6)	4198(2)	- 6127(3)	943(1)	31(1)
C(7)	5966(2)	- 3596(3)	2849(1)	27(1)
C(8)	5474(2)	- 1376(3)	3089(1)	30(1)
C(9)	7186(2)	- 4767(3)	3260(1)	29(1)

[a] Equivalent isotropic U defined as one third of the trace of the orthogonalized U_{ij} tensor

were obtained (MOPAC program, AM1), which were analyzed by the HYPER program [20]. Experimental X-ray geometries for molecules I and II were used in the calculations.

3. Results and discussion

Fig. 2 shows the crystal structures of molecules A and B of compound I which was synthesized from

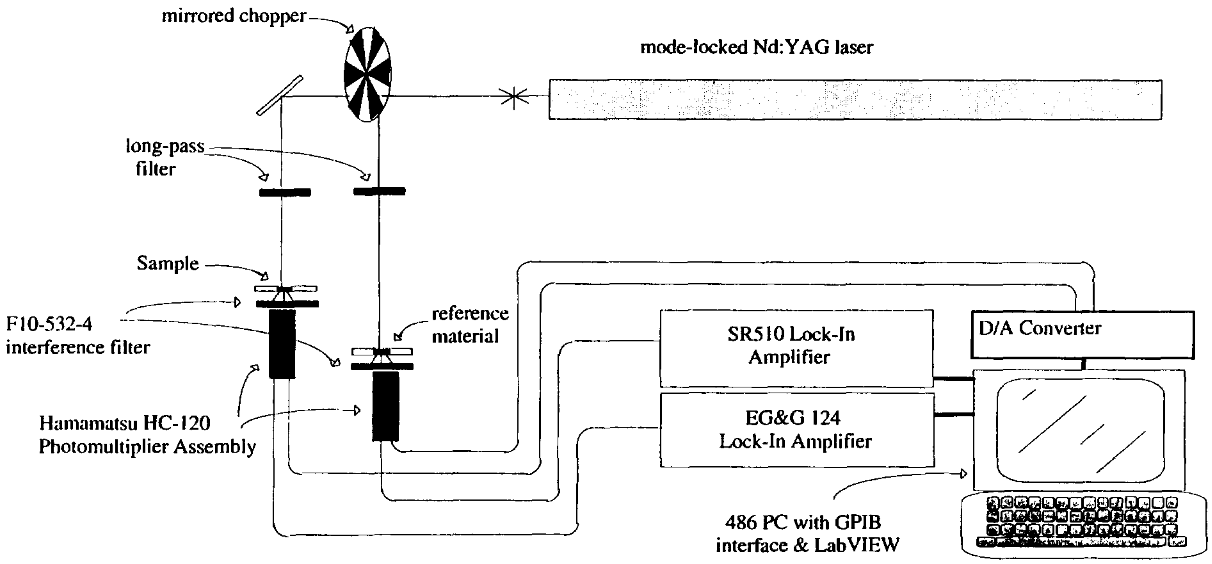

Fig. 1. Experimental configuration for Kurtz powder measurements.

Table 4
Bond lengths (Å), bond angles (°), and base torsion angles (°) in structure I

O(21)–N(20)	1.18(1)	N(20′)–O(21′)	1.11(1)
O(22)–N(20)	1.205(9)	O(22′)–N(20′)	1.22(1)
N(7)–N(8)	1.285(7)	N(7′)–N(8′)	1.271(7)
N(7)–C(1)	1.411(8)	N(7′)–C(1′)	1.424(8)
N(8)–C(9)	1.366(8)	N(8′)–C(9′)	1.369(8)
N(11)–C(10)	1.167(7)	N(11′)–C(10′)	1.152(7)
N(13)–C(12)	1.319(7)	N(13′)–C(12′)	1.336(8)
N(14)–C(12)	1.336(8)	N(14′)–C(12′)	1.319(8)
N(14)–C(15)	1.475(8)	N(14′)–C(15′)	1.467(9)
N(14)–C(19)	1.478(9)	N(14′)–C(19′)	1.477(9)
N(20)–C(2)	1.49(1)	N(20′)–C(2′)	1.46(1)
C(1)–C(2)	1.383(9)	C(1′)–C(2′)	1.388(9)
C(1)–C(6)	1.400(9)	C(1′)–C(6′)	1.406(9)
C(2)–C(3)	1.39(1)	C(2′)–C(3′)	1.40(1)
C(3)–C(4)	1.37(1)	C(3′)–C(4′)	1.37(1)
C(4)–C(5)	1.39(1)	C(4′)–C(5′)	1.38(1)
C(5)–C(6)	1.39(1)	C(5′)–C(6′)	1.37(1)
C(9)–C(10)	1.399(8)	C(9′)–C(10′)	1.421(8)
C(9)–C(12)	1.438(8)	C(9′)–C(12′)	1.431(8)
C(15)–C(16)	1.497(9)	C(15′)–C(16′)	1.534(9)
C(16)–O(17)	1.422(9)	C(16')–O(17')	1.425(9)
C(18)–O(17)	1.415(8)	O(17')–C(18')	1.426(9)
C(18)–C(19)	1.507(9)	C(18′)–C(19′)	1.50(1)
C(16)–O(17)–C(18)	110.0(4)	C(16′)–O(17′)–C(18′)	109.6(5)
N(8)–N(7)–C(1)	112.9(5)	N(8′)–N(7′)–C(1′)	111.8(4)
N(7)–N(8)–C(9)	115.0(5)	N(7′)–N(8′)–C(9′)	115.9(4)
C(12)–N(14)–C(15)	125.1(5)	C(12′)–N(14′)–C(15′)	124.9(5)
C(12)–N(14)–C(19)	122.8(5)	C(12′)–N(14′)–C(19′)	123.0(5)
C(15)–N(14)–C(19)	111.4(5)	C(15′)–N(14′)–C(19′)	112.0(5)
O(21)–N(20)–O(22)	126.4(9)	O(21′)–N(20′)–O(22′)	116.2(9)
O(21)–N(20)–C(2)	118.4(7)	O(21′)–N(20′)–C(2′)	125.3(8)
O(22)–N(20)–C(2)	115.0(8)	O(22′)–N(20′)–C(2′)	118.3(8)
N(7)–C(1)–C(2)	117.8(5)	N(7′)–C(1′)–C(2′)	117.5(5)
N(7)–C(1)–C(6)	125.2(6)	N(7′)–C(1′)–C(6′)	125.9(6)
C(2)–C(1)–C(6)	116.8(6)	C(2′)–C(1′)–C(6′)	116.5(6)
N(20)–C(2)–C(1)	118.4(6)	N(20′)–C(2′)–C(1′)	119.1(6)
N(20)–C(2)–C(3)	118.2(6)	N(20′)–C(2′)–C(3′)1	117.3(6)
C(1)–C(2)–C(3)	123.3(6)	C(1′)–C(2′)–C(3′)	123.6(6)
C(2)–C(3)–C(4)	119.3(7)	C(2′)–C(3′)–C(4′)	117.7(7)
C(3)–C(4)–C(5)	118.8(7)	C(3′)–C(4′)–C(5′)	120.4(7)
C(4)–C(5)–C(6)	121.6(7)	C(4′)–C(5′)–C(6′)	121.4(7)
C(1)–C(6)–C(5)	120.2(6)	C(1′)–C(6′)–C(5′)	120.4(6)
N(8)–C(9)–C(10)	120.5(5)	N(8′)–C(9′)–C(10′)	119.9(5)
N(8)–C(9)–C(12)	116.4(5)	N(8′)–C(9′)–C(12′)	117.2(5)
C(10)–C(9)–C(12)	122.3(5)	C(10′)–C(9′)–C(12′)	122.3(5)
N(11)–C(10)–C(9)	177.2(7)	N(11′)–C(10′)–C(9′)	176.2(7)
N(13)–C(12)–N(14)	120.0(5)	N(13′)–C(12′)–N(14′)	120.3(5)
N(13)–C(12)–C(9)	118.6(5)	N(13′)–C(12′)–C(9′)	116.8(6)
N(14)–C(12)–C(9)	121.3(5)	N(14′)–C(12′)–C(9′)	122.9(5)
N(14)–C(15)–C(16)	110.0(5)	N(14′)–C(15′)–C(16′)	108.3(5)
O(17)–C(16)–C(15)	110.3(5)	O(17′)–C(16′)–C(15′)	111.8(6)
O(17)–C(18)–C(19)	112.1(6)	O(17′)–C(18′)–C(19′)	111.0(5)
N(14)–C(19)–C(18)	108.7(5)	N(14′)–C(19′)–C(18′)	109.1(6)

Table 4
(*continued*)

N(7)-C(1)-C(2)-N(20)	- 8.5(8)	N(7')-C(1')-C(2')-N(20')	3.6(8)
O(21)-N(20)-C(2)-C(1)	- 67.4(1.0)	O(21')-N(20')-C(2')-C(1')	95.8(1.2)
O(21)-N(20)-C(2)-C(3)	110.5(9)	O(21')-N(20')-C(2')-C(3')	- 82.4(1.2)
O(22)-N(20)-C(2)-C(1)	116.9(9)	O(22')-N(20')-C(2')-C(1')	- 78.1(1.0)
O(22)-N(20)-C(2)-C(3)	- 65.3(1.0)	O(22')-N(20')-C(2')-C(3')	103.8(1.0)
N(8)-N(7)-C(1)-C(2)	163.5(5)	N(8')-N(7')-C(1')-C(2')	- 165.8(5)
N(8)-N(7)-C(1)-C(6)	- 21.1(8)	N(8')-N(7')-C(1')-C(6')	17.7(8)
C(1)-N(7)-N(8)-C(9)	176.8(5)	C(1')-N(7')-N(8')-C(9')	- 177.7(5)
N(7)-N(8)-C(9)-C(10)	- 9.0(8)	N(7')-N(8')-C(9')-C(10')	5.1(8)
N(7)-N(8)-C(9)-C(12)	- 179.5(5)	N(7')-N(8')-C(9')-C(12')	176.9(5)
N(8)-C(9)-C(10)-N(11)	- 70.5(2.0)	N(8')-C(9')-C(10')-N(11')	41.8(2.0)
N(8)-C(9)-C(12)-N(13)	19.2(7)	N(8')-C(9')-C(12')-N(13')	- 18.7(8)
N(8)-C(9)-C(12)-N(14)	- 160.9(5)	C(8')-C(9')-C(12')-N(14')	163.7(5)
C(10)-C(9)-C(12)-N(13)	- 151.1(6)	C(10')-C(9')-C(12')-N(13')	152.9(6)
C(10)-C(9)-C(12)-N(14)	28.7(8)	C(10')-C(9')-C(12')-N(14')	- 24.8(9)
C(12)-C(9)-C(10)-N(11)	99.5(2.0)	C(12')-C(9')-C(10')-N(11')	- 129.5(2.0)
C(15)-N(14)-C(12)-C(9)	29.6(8)	C(15')-N(14')-C(12')-C(9')	- 23.7(8)
C(15)-N(14)-C(12)-N)(13)	- 150.6(5)	C(15')-N(14')-C(12')-N(13')	158.7(6)
C(19)-N(14)-C(12)-N(13)	18.7(8)	C(19')-N(14')-C(12')-N(13')	- 16.8(8)
C(12)-N(14)-C(15)-C(16)	- 134.7(6)	C(12')-N(14')-C(15')-C(16')	- 121.6(6)
C(19)-N(14)-C(15)-C(16)	54.9(6)	C(19')-N(14')-C(15')-C(16')	54.3(7)
C(12)-N(14)-C(19)-C(18)	136.2(6)	C(12')-N(14')-C(19')-C(18')	119.9(6)
C(15)-N(14)-C(19)-C(18)	- 53.2(6)	C(15')-N(14')-C(19')-C(18')	- 56.2(6)
N(14)-C(15)-C(16)-O(17)	- 58.1(7)	N(14')-C(15')-C(16')-O(17')	- 56.5(7)
C(16)-O(17)-C(18)-C(19)	- 61.2(7)	C(16')-O(17')-C(18')-C(19')	- 61.3(7)
O(17)-C(18)-C(19)-N(14)	56.6(7)	O(17')-C(18')-C(19')-N(14')	58.8(7)
C(18)-O(17)-C(16)-C(15)	61.1(7)	C(18')-O(17')-C(16')-C(15')	60.3(7)
C(19)-N(14)-C(12)-C(9)	- 161.1(5)	C(19')-N(14')-C(12')-C(9')	160.7(5)

compound II. The structure of molecule II in the crystal is shown on Fig. 3. Geometrical parameters of molecules I and II are listed in Tables 4 and 5.

Crystals of compound I are built with two systems of symmetrically independent molecules (A and B), which differ with regard to the relative orientation of the morpholine substituent (torsion angles C(15)N(14)C(12)C(9) 29.6(8) and − 23.7(8)°, and

Table 5
Bond lengths (Å), and bond angles (°) in molecule II

O(1)-N(1)	1.239(2)	N(4)-C(8)	1.135(2)	C(3)-C(4)	1.364(3)
O(2)-N(1)	1.221(2)	N(5) C(9)	1.145(2)	C(4)-C(5)	1.385(2)
N(1)-C(2)	1.447(2)	C(1)-C(2)	1.402(2)	C(5)-C(6)	1.379(2)
N(2)-N(3)	1.311(2)	C(1)-C(6)	1.388(2)	C(7)-C(8)	1.430(2)
N(2)-C(1)	1.396(2)	C(2)-C(3)	1.395(2)	C(7)-C(9)	1.427(2)
N(3)-C(7)	1.308(2)				
O(1)-N(1)-O(2)	121.8(1)	C(1)-C(2)-C(3)	120.7(1)		
O(1)-N(1)-C(2)	119.7(1)	C(2)-C(3)-C(4)	120.1(1)		
O(2)-N(1)-C(2)	118.6(1)	C(3)-C(4)-C(5)	119.6(1)		
N(3)-N(2)-C(1)	120.7(1)	C(4)-C(5)-C(6)	121.0(2)		
N(2)-N(3)-C(7)	116.3(1)	C(1)-C(6)-C(5)	120.4(1)		
N(2)-C(1)-C(2)	121.1(1)	N(3)-C(7)-C(8)	122.6(1)		
N(2)-C(1)-C(6)	120.7(1)	N(3)-C(7)-C(9)	119.2(1)		
C(2)-C(1)-C(6)	118.2(1)	C(8)-C(7)-C(9)	118.2(1)		
N(1)-C(2)-C(1)	122.5(1)	N(4)-C(8)-C(7)	174.4(2)		
N(1)-C(2)-C(3)	116.8(1)	N(5)-C(9)-C(7)	175.6(2)		

Table 6
Five top-list energies of C_i, C_2 and parallel dimers (kcal mol^{-1}) for molecules I and II

Molecule I			Molecule II		
C_i	C_2	Parallel	C_i	C_2	Parallel
59.54	66.40	62.55	26.43	27.87	27.92
59.72	66.58	62.64	26.51	27.94	27.95
59.87	66.72	62.73	26.60	28.00	27.98
59.97	66.81	62.83	26.69	28.10	28.00
60.13	66.94	63.00	26.84	28.21	28.01

C(12)N(14)C(15)C(16) − 134.7(6) and − 121.6(6)°, in molecules A and B, respectively). Molecules of compound I belong to azo-form according to the results of X-ray analysis. Intramolecular steric hindrance leads to a NO_2-group rotation relative to the plane of the phenyl ring (dihedral angles between these planes in molecules A and B are 66.2 and 100.4° respectively). Dihedral angles between the plane of the phenyl ring and the plane of the conjugated C(1)–N(7)=N(8)–C(9)=C(12) fragment [mean atom deviation from this plane is ± 0.015 (A) and ± 0.016 Å (B)] are 18.9 and 13.7° in molecules A and B respectively. The deviations from the mean molecular plane of CN- and NH_2-substituents are even

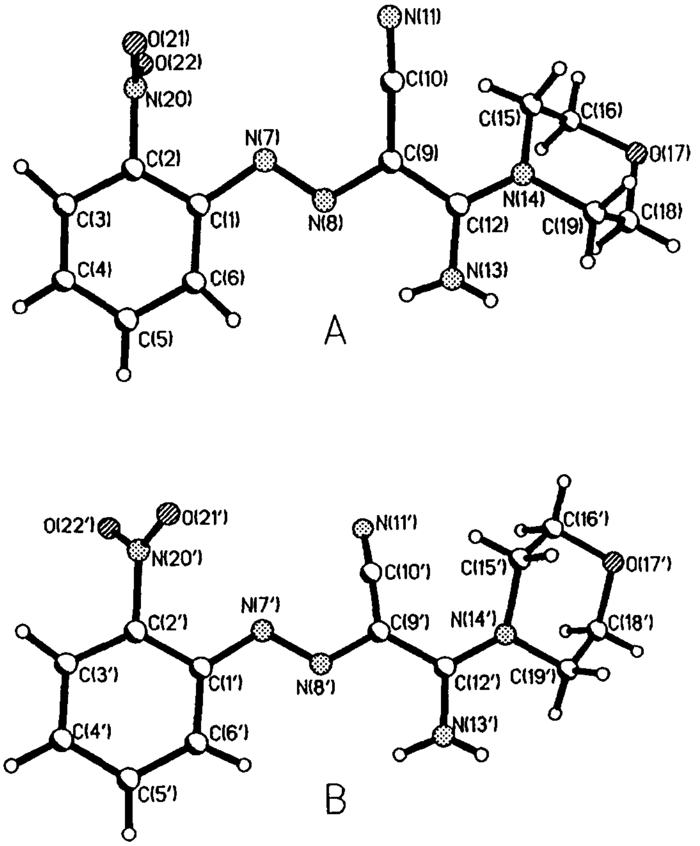

Fig. 2. Structure of symmetrically independent molecules A and B in the crystal I.

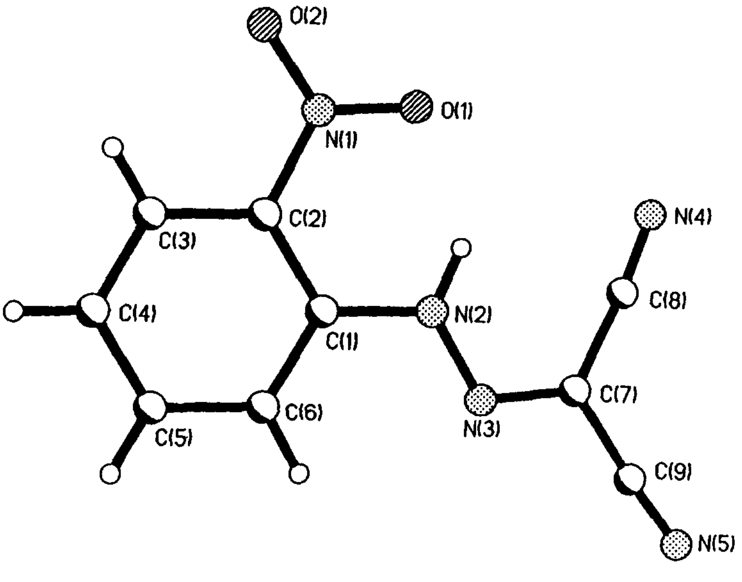

Fig. 3. Structure of molecule II in crystal.

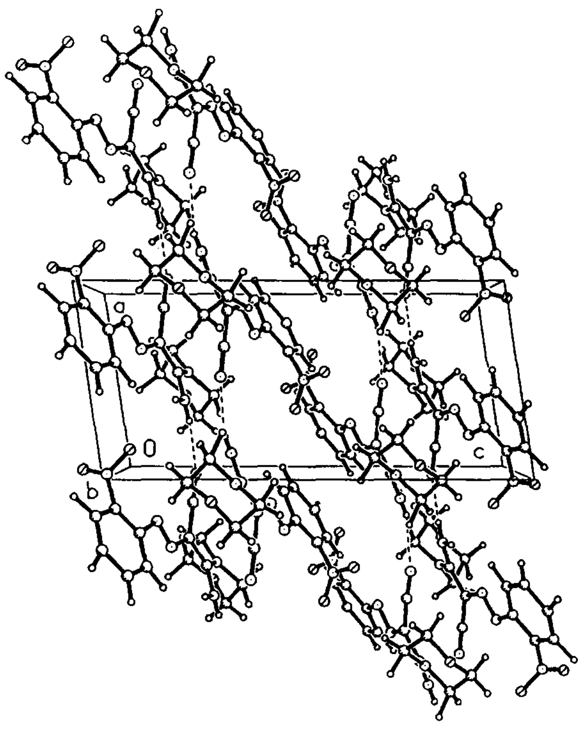

Fig. 4. Projection of molecular packing in crystal I along *b* axis.

more significant (Fig. 2, Table 4). We note a pronounced conjugation between the double C(9) = C(12) bond and neighboring nitrogen atoms, which is characterized by deviation of the corresponding bond length from standard values [21].

Molecules A and B in a crystal form separate chains (···A···A, ···B···B) parallel to the *a* direction, linked with hydrogen bonds between NH_2 and CN groups (Fig. 4). Geometrical parameters of hydrogen bonds are as follows: N(13)–H(13a)···N(11) ($x-1$, y, z) [N(13)–N(11) 2.975(8), N(13)–H(13a) 0.76(6), H(13a)···N(11) 2.25(8) Å, angle N(13)–H(13a)···N(11) 159(1)°]; N(13′)–H(13d)–N(11′) ($1+x$, y, z) [N(13′)···N(11′) 2.951(8), N(13′)–H(13d) 0.92(6), H(13d)···N(11′) 2.06(8) Å, angle N(13′)–H(13d)···N(11′) 162(1)°]. The geometrical parameters of molecule I (bond lengths and bond angles) according to MM calculations are close to the values found from X-ray analysis. The molecular conformation of isolated molecules differ from those for molecules I (A and B) in the crystal. According to calculations, molecule I is nearly planar, except for the NO_2 and morpholine groups. We suggest that nonplanarity of these molecules in the crystal is caused by the crystal environment, especially by intermolecular hydrogen bond formation.

Molecule II (Fig. 3) is nearly planar. It is possible to describe it as consisting of four nearly planar fragments, such as, the phenyl ring (plane A), atoms C(1), N(2), N(3), and C(7) (plane B, mean deviation from the plane (0.038 Å), and atoms N(4), C(8), C(7), C(9), and N(5) (plane C, mean deviation from the plane (0.009 Å), and the NO_2-group (plane D). Dihedral angles A/B and B/C and A/D are equal to 3.7, 7.2 and 6.7°. The reason for the nearly coplanar nitro-group orientation is the strong intramolecular hydrogen bond between the O atom of the nitro-group and the H atom of the amino-group. Parameters of the N(2)–H(2)···O(1) hydrogen bond are as follow: N(2)···O(1) 2.585(2), N(2)–H(2) 0.89(2) H(2)···O(1) 1.87 Å, angle N(2)–H(2)···O(1) 135(1)°. We should note that one of the cyano-groups, which has close non-bonded contact with the H atom of the amino-group (C(8)···H(2) 2.34(2) Å) is not linear. The bond angle C(7)C(8)N(4) is equal to 174.4(2)°.

The planar structure of molecule II is favorable to some extent for π-conjugation, which is demonstrated by comparison of the alternation of the bond lengths (Table 5) with standard values [15]. Two short intermolecular contacts in structure II were found: N(4)···N(1) $(0.5-x, 0.5+x, 0.5-z)$ 2.957(2) Å, and N(4)···C(2) $(0.5-x, 0.5+x, 0.5-z)$ 3.098(3) Å.

The most interesting characteristic of the potential NLO compound is the crystal space group and type of molecular packing. In order to find a correlation between molecular structure and space group in our previous work [8], we used calculations of the structure and energy of molecular dimers as a test. To some extent this test characterizes the first stage of molecular nucleation during crystallization process [6,7]. Calculations for dimers of molecules I and II show (Table 6) that for these molecules centrosymmetric dimers are preferable to dimers of C_2 symmetry or dimers with parallel molecular orientation. It should be mentioned that for molecules I, the preference for centrosymmetric dimer formation is significant (ca. 3 kcal mol^{-1}). Several top-list "C_i" dimers of molecule II do not have ideal C_i symmetry, but all of them are nearly centrosymmetric and characterized by antiparallel molecular orientation. These results suggest that both molecules should exhibit a centrosymmetric space group. Indeed, crystal II is characterized by a centrosymmetric space group (Table 1). The situation with crystal I is not the same. The structure of calculated C_i dimers formed by molecules I (Fig. 5(a)) and dimers found in crystal I (Fig. 5(b)) is very close. But in the crystal these dimers have only approximate C_i symmetry (they are formed by symmetrically independent molecules A and B, whose conformation is slightly different, Table 4). Crystals of compound I belong to the acentric space group ($P2_1$, Table 1), but the molecular pattern in this structure is quite close to the centrosymmetric one.

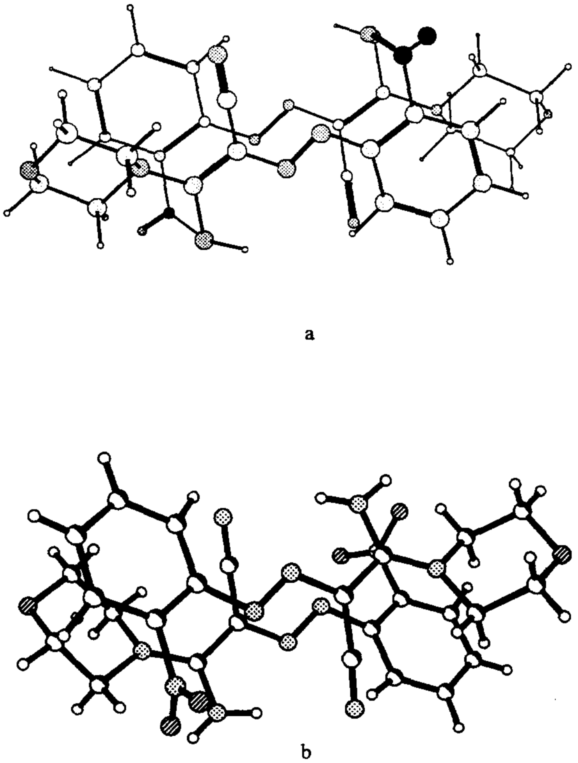

Fig. 5. (a) Calculated and (b) X-ray structure of molecular dimers with approximate C_i symmetry.

The coexistence of two or more symmetrically independent molecules in one crystal is quite rare, and it is obvious that this situation cannot be predicted with such a simple test as a dimer structure formation. Nevertheless, even for compound I the test appeared to be very useful. It is understandable that the presence of pseudo-centrosymmetric dimers (even in an acentric crystal structure) is not desirable for SHG.

The calculated static field molecular hyperpolarizability (β) is equal to $67.96 \pm 0.02 \times 10^{-51}$ C m^3 V^{-2} for compound I. It is approximately two times larger

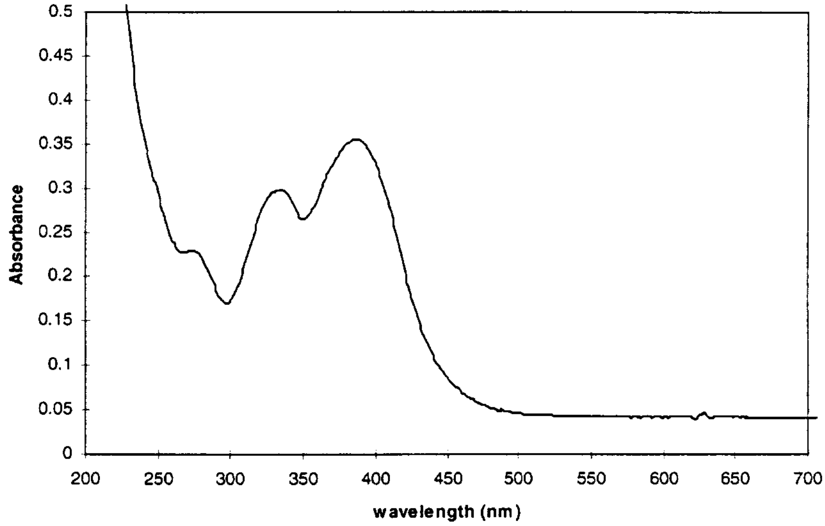

Fig. 6. Electronic absorption spectra of compound I in ethanol solution.

than the value calculated in the same approximation for the extensively studied SHG compound COANP [22,23]. One cannot anticipate a large hyperpolarizability value for compound II according to its chemical structure. The value of β calculated for molecule II is $8.48 \pm 0.01 \times 10^{-51}$ C m^3 V^{-2}. Unfortunately, even for compound I we could not expect SHG in the crystal because of unfavorable molecular crystal packing. Nevertheless this compound could be useful for SHG in solution or a polymer matrix. Conformational calculations and experimental results (the coexistence of two symmetrically independent molecules with different conformations in one crystal) suggest that this compound, because of its molecular flexibility, can probably form a glass state, as was found for COANP [22,23].

The electronic absorption spectrum of compound I (Fig. 6) shows a prominent absorption peak in the blue region at 387 nm that extends into the visible, accounting for the color of the material. The spectrum is shown in Fig. 6. The region of absorption of compound I should not prevent detection of SGH by an Nd:YAG laser.

Experimental powder SHG measurements of compound I are in agreement with our predictions based on molecular dimer formation found as a result of crystal structure analysis and calculations and did not show SHG. The sensitivity of the ratiometric technique used permitted discrimination to about one part in one thousand relative to MNA. The measured second harmonic output ratio was 1.4×10^{-3}, i.e. a null result for this experiment.

These results once more show the importance not only of space group, but also the relative molecular orientation in the crystal phase for demonstrating special physical properties, namely SHG. A simple computational test, demonstrating the type of preferable molecular dimer, appears to be useful in establishing the property–structure interconnection.

Acknowledgements

The authors are grateful to Dr. Norman L. Allinger for the use of MM3 program, and Dr. Beatriz Cardelino and Dr. Craig E. Moore for the use of their program for hyperpolarizability calculations. The project was supported in part by NASA Alliance for Nonlinear Optics, Grant NASW-4078.

References

[1] D.S. Chelma, J. Zyss (eds.), Nonlinear Optical Properties of Organic Molecules and Crystals, vol. 1, Academic Press, Orlando, FL, 1987.

[2] D.R. Kanis, M.A. Ratner, T.J. Marks, Chem. Rev. 94 (1994) 195.

[3] T. Tsunekawa, K. Yamaguchi, J. Chem. Phys. 96 (1992) 10268.

[4] A. Gavezotti, Acc. Chem. Res. 27 (1994) 309.

[5] J.J. Wolf, Angw. Chem. Int. Ed. Engl. 35 (1996) 2195.

[6] Y. Itoh, K. Oono, M. Isogai, A. Kakuta, Mol. Cryst. Liq. Cryst. 170 (1989) 259.

[7] Y. Itoh, K. Oono, M. Isogai, A. Kakuta, SPIE, Nonlinear Opt. Mater. 1017 (1988) 127.

[8] M.Yu. Antipin, T.A. Barr, B. Cardelino, R.D. Clark, C.E. Moore, T. Myers, B. Penn, M. Romero, M. Sangadasa, T.V. Timofeeva, J. Phys. Chem. B 101 (1997) 2770.

[9] V.K. Promonenkov, A.M. Shestopalov, Yu.A. Sharanin, Itogi Nauki i Tekhniki VINITI, Ser. Org. Khim, Moscow 17 (1989) 231–252. (in Russian).

[10] F. Freeman, Syntesis 21 (1981) 952.

[11] K.K.Venters,U.Ya. Mikstais, A.E. Pengerotye, G.F. Kumerov, Izv. Akad. Nauk Latv. SSR., Ser. Khim. 1 (1990) 100.

[12] W. Robinson and G.M. Sheldrick, in: Crystallographic Computing—Techniques and New Technologies, Oxford University Press, Oxford, 1988, p. 366.

[13] S.K. Kurtz, T.T. Perry, J. Appl. Phys. 39 (1968) 3798.

[14] N.L. Allinger, Y.H. Yuh, J.-H. Lii, J. Am. Chem. Soc. 111 (1989) 8551.

[15] J.-H. Lii, N.L. Allinger, J. Am. Chem. Soc. 111 (1989) 8566.

[16] M.J. Saunders, J. Am. Chem. Soc. 109 (1987) 3150.

[17] B.H. Cardelino, C.E. Moore, D.O. Frazier, J. Phys. Chem. A 101 (1997) 2207.

[18] M.J.S. Dewar, J.J.P. Stewart, Chem. Phys. Lett. 111 (1984) 416.

[19] H.A. Kurtz, J.J.P. Stewart, K.M. Dieter, J. Comput. Chem. 11 (1990) 82.

[20] B.H. Cardelino, C.E. Moore, R.E. Stickel, J. Phys. Chem. 95 (1991) 8645.

[21] F.H. Allen, O. Kennard, D.G. Watson, L. Brammer, A.G. Orpen, R. Taylor, J. Chem. Soc., Perkin Trans. 2, (1987) S1.

[22] P. Guenter, Ch. Bosshard, K. Sutter, H. Arend, G. Chapius, R.J. Tweig, D. Dobrowolski, Appl. Phys. Lett. 50 (1987) 486.

[23] M. Eich, H. Looser, Do Y. Yoon, R. Tweig, G. Bjorklund, J.C. Baumer, J. Opt. Soc. Am. 6 (1989) 1590.